

Electrical transport in $\text{La}_{1-x}\text{Sr}_x\text{CoO}_3$ ($0.03 \leq x \leq 0.07$) below 60 K

E Iguchi, K Ueda and H Nakatsugawa

Materials Science, Department of Mechanical Engineering and Materials Science, Faculty of Engineering, Yokohama National University, Tokiwadai, Hodogaya-Ku, Yokohama 240-8501, Japan

Received 15 April 1998, in final form 2 June 1998

Abstract. The electrical transport properties of $\text{La}_{1-x}\text{Sr}_x\text{CoO}_3$ ($0.03 \leq x \leq 0.07$) have been investigated using complex-plane impedance analysis and dielectric measurements with measurements of four-probe dc conductivities and magnetic susceptibilities. The temperature dependencies of the bulk conductivities obtained by impedance analysis, and dielectric relaxation processes provide evidence of the hopping conduction below 60 K, which is remarkably different from the hopping conduction in LaCoO_3 , despite the degree of doping with Sr being very small. The features in the low-doping range are: (i) the emergence of the hopping conduction at markedly lower temperatures in comparison with the case for non-doped LaCoO_3 ; (ii) the abrupt reduction of the activation energy required for the conduction, 0.042 eV at $x = 0.03$ to 0.021 eV at $x = 0.07$, from 0.34 eV for LaCoO_3 ; and (iii) a progressive decrease in the activation energy with increasing x . The difference in conduction behaviour between $\text{La}_{1-x}\text{Sr}_x\text{CoO}_3$ and LaCoO_3 is due to the alternation of the spin state of Co^{3+} caused by the Sr doping. The results have been discussed in terms of a process of hopping of small polarons localized by the electron–lattice interaction in tandem with the electron–magnon interaction.

1. Introduction

In comparison with other LaMO_3 compounds ($M = \text{Ti}, \text{V}, \text{Cr}, \text{Mn}, \text{Fe}, \text{Ni}$) which are well known as strongly correlated systems [1–14], LaCoO_3 has been particularly extensively studied; it exhibits the characteristic behaviour associated with the metal–insulator transition as well as a spin-state transition due to a change in the spin state of the Co ions [15–27]. The main feature of interest in LaCoO_3 has been the magnetism due to the spin-state transition, which is closely related to the electronic structure. However, conduction measurement is also indispensable for elucidating the electronic structure, because transport properties and the nature of the carriers depend very sensitively upon the electronic structure. We have proposed that conduction occurs due to a process of hopping of small polarons of holes which are created by electron excitation across the band gap of 0.2 eV over the temperature interval $120 \text{ K} \leq T \leq 300 \text{ K}$ in LaCoO_3 [28].

Recently, Saitoh *et al* [29] have studied the electronic structure of LaCoO_3 by photoemission spectroscopy and x-ray absorption spectroscopy (XAS). Since the ground state of LaCoO_3 in the low-spin Co^{III} ($t_{2g}^6 e_g^0$) state is found to have heavily mixed ($\sim 30\%$ d^6 , $\sim 50\%$ $d^7 \underline{L}$, and $\sim 20\%$ $d^8 \underline{L}^2$) character, the magnetic susceptibility has been analysed for various level orderings of the low-spin Co^{III} ($t_{2g}^6 e_g^0$), the intermediate-spin Co^{III} ($t_{2g}^5 e_g^1$), and the high-spin Co^{3+} ($t_{2g}^4 e_g^2$) states. From the cluster-model analysis of the spectra as well as

the analysis of the magnetic susceptibility, the magnetic transition in LaCoO_3 at about 90 K seems most likely to be due to a transition from a low-spin to an intermediate-spin state.

Substitution of Sr^{2+} for La^{3+} in LaCoO_3 brings about remarkable changes in the system [30–33]. Electrical neutrality requires one positive hole per Sr^{2+} ion. On the basis of the valence of the Co ions, then, LaCoO_3 is a monovalent system, while $\text{La}_{1-x}\text{Sr}_x\text{CoO}_3$ is a mixed-valence system. Besides the spin-glass phases in $\text{La}_{1-x}\text{Sr}_x\text{CoO}_3$ ($x < 0.2$) at low temperatures [34, 35], lightly Sr-doped compounds exhibit extrinsic magnetic properties significantly different from those of LaCoO_3 . The major changes are: (i) the spin state of the Co ions evolves toward the intermediate-spin state Co^{iii} at $x = 0.08$ from the low-spin state Co^{iii} at $x = 0$ at low temperatures [25, 36]; and (ii) the susceptibility drop due to the transition from a high-spin to a low-spin state which is characteristic of LaCoO_3 is suppressed, and instead a Curie-like contribution is predominant even in the $x = 0.005$ compound [26]. These results indicate a change in the electronic structure, and thus the conduction behaviour of lightly Sr-doped compounds is expected to differ considerably from that of LaCoO_3 [28]. Though the main interest in $\text{La}_{1-x}\text{Sr}_x\text{CoO}_3$ has been in the magnetic properties, which are very sensitive to the electronic structure [30–32, 37–39], it is of great importance to elucidate the electrical transport associated with the change in the electronic structure.

Recently, Señarís-Rodríguez and Goodenough [35] reported on magnetic and transport properties of $\text{La}_{1-x}\text{Sr}_x\text{CoO}_3$ ($0 < x \leq 0.50$). For $x \leq 0.20$, they argue that a process of hopping of small polarons of holes dominates the electrical transport over the temperature interval $110 \text{ K} \leq T \leq 350 \text{ K}$, but that the activation energies required for the transport reduce remarkably to 0.08 eV at $x = 0.025$ –0.04 eV at $x = 0.150$, from 0.34 eV for LaCoO_3 [28]. Such an abrupt reduction of the activation energy even at very small x is subject to debate. Measuring magnetic susceptibilities for lightly hole-doped specimens with $x \leq 0.01$, Yamaguchi *et al* [26] suggest that hole doping in the low-spin ground state of LaCoO_3 leads to the formation of localized magnetic polarons, i.e., spin polarons associated with a strong exchange interaction between a 2p hole and 3d spins. Therefore two candidates for the carrier have been proposed for the low-doping range, i.e., a small polaron and a spin polaron. Below 110 K, Señarís-Rodríguez and Goodenough [35] reported another type of hopping conduction. This is also a subject of debate.

An attempt to account for these issues, i.e., the large reduction of the activation energy and the nature of the majority carrier, should be made. An attempt such as this requires a detailed measurement of the electrical transport as well as magnetic experiments, because the conduction mechanism participates directly in these phenomena due to the change in the electronic structure caused by a light Sr doping.

In the case where $x > 0.1$, the relations between the magnetic structures and the spin states of Co ions have been investigated in detail by means of neutron diffraction measurements, ac magnetic susceptibility studies, resistivity measurements, and so on [40–42]. Fundamentally, the paramagnetic states of Co ions in the predominantly diamagnetic low-spin state in LaCoO_3 are stable in this composition region. The core $S = 1$ spin of trivalent Co coupled ferromagnetically to an itinerant e_g electron by the double-exchange $\text{Co}^{4+}\text{--O--Co}^{3+}$ mechanism seems very likely to play an important role in the electronic transport behaviour. These results for $x > 0.1$ should be helpful in the elucidation of the electrical transport in the light-hole-doping regime, i.e., for $x \leq 0.07$, which is however expected to be a regime in which behaviour somewhat different from that of the heavily doped materials is exhibited.

As described in the literature, in the materials in which hopping conduction dominates the electrical transport, dielectric measurements provide important information, because

a hopping process has a high probability of involving a dielectric relaxation [43–53]. Thus a combination of conductivity and dielectric measurements is very useful in the investigation of hopping conduction. The ‘conduction’ described here is bulk conduction. The grain boundaries in a sintered LaCoO_3 specimen interfere with the study of the transport phenomenon [28]. While the use of single crystals certainly alleviates most problems, complex-plane impedance analysis can distinguish bulk conduction from other types of conduction such as that across the grain boundaries even if a polycrystalline ceramic specimen is employed [54–57]. Impedance analysis, then, provides very important results, leading directly to the real features of the electrical transport in $\text{La}_{1-x}\text{Sr}_x\text{CoO}_3$ materials.

Since the discovery of high- T_c superconductivity in the layer perovskite $\text{La}_{2-x}\text{Ba}_x\text{CuO}_4$ [58], the investigation of polarons including spin polarons has attracted markedly increased attention, because polaronic conduction plays an important role in electrical transport in strongly correlated oxides. Although there are many ways of addressing polaron dynamics, dielectric properties can also provide important information.

Motivated by these factors, in the present report we will elucidate the electrical transport in $\text{La}_{1-x}\text{Sr}_x\text{CoO}_3$ materials following a somewhat different route from previous reports, which have concentrated predominantly upon magnetic properties, using a combination of impedance analysis and dielectric measurements with dc conductivity measurements. Since the upper-limit temperature at which impedance analysis is possible decreases from 60 K at $x = 0.03$ to 30 K at $x = 0.07$, the present study treats the low-doping range of $0.03 \leq x \leq 0.07$ at rather low temperatures.

2. Experimental details

Three sorts of $\text{La}_{1-x}\text{Sr}_x\text{CoO}_3$ specimen (with $x = 0.03, 0.05,$ and 0.07) were prepared by the solid-state reaction method. The appropriate mixtures of La_2O_3 , Co_3O_4 , and SrCO_3 powders (4N) were ground and calcined in air at 1100 °C for one day, and then, after being mixed very carefully, calcined again under the same conditions for two days. The second process was then repeated. The powder was then pressed into pellets and finally sintered at 1350 °C for one day, and then cooled at a rate of approximately 80 °C h⁻¹ to room temperature. The last heating process was carried out in pure flowing oxygen. This cooling rate is nearly equal to those employed by Señaris-Rodríguez and Goodenough (60 °C h⁻¹) [35] and Golovanov *et al* (100 °C h⁻¹) [59], but Itoh *et al* employed a very slow rate (100 °C per day) [34]. However, our preparation process reproduced specimens with the same characteristics.

Every specimen was confirmed to be single phase with rhombohedrally distorted perovskite structure by a Cu K α x-ray powder diffraction analysis. The hexagonal cell parameters were calculated from x-ray diffraction patterns at room temperature: $a_H = 5.446$ Å and $c_H = 13.107$ Å for $x = 0.03$, $a_H = 5.446$ Å and $c_H = 13.114$ Å for $x = 0.05$, and $a_H = 5.447$ Å and $c_H = 13.123$ Å for $x = 0.07$. The oxygen deficiency in $\text{La}_{1-x}\text{Sr}_x\text{CoO}_{3-\delta}$ should be considered when $x > 0.5$ unless specimens are prepared under high oxygen pressures [38, 39], but δ in $\text{La}_{1-x}\text{Sr}_x\text{CoO}_{3-\delta}$ for the present specimens must be negligibly small because $x \leq 0.07$. The grain size of the specimens was found to be ~ 8 μm on average by scanning electron microscope studies. The densities of the specimens were about 90% of the theoretical values.

The capacitance and impedance were obtained as functions of the temperature above around 15 K by the four-terminal pair ac impedance measurement method, using an HP 4284A Precision LCR meter with a frequency range of 100 Hz to 1 MHz. The measured

values of the capacitance and impedance were corrected by calibrating the capacitance and resistance of the leads to zero. The flat surfaces of the specimens were coated with an In–Ga alloy in the ratio 7:3 by a rubbing technique applied to the electrodes. Evaporated gold was also used for the electrode, but no significant difference was found. In order to check for Maxwell–Wagner-type polarization, capacitance measurements were carried out at 27 K and 38 K in the frequency range 1 kHz–1 MHz by changing the thickness of the specimen with $x = 0.05$ from 1.0 mm to 0.5 mm, but the dielectric constants were found to be independent of the thickness. Hence, Maxwell–Wagner-type polarization is excluded.

A Keithley 619 resistance bridge, an Advantest TR 6871 digital multimeter, and an Advantest R 6161 power supply were used for the dc conductivity measurements by the four-probe method. A copper–constantan thermocouple pre-calibrated at 4.2, 77, and 273 K was used for the temperature measurements.

Although a specimen with $x = 0.09$ was produced, impedance analysis and dielectric measurements have required temperatures lower than 15 K.

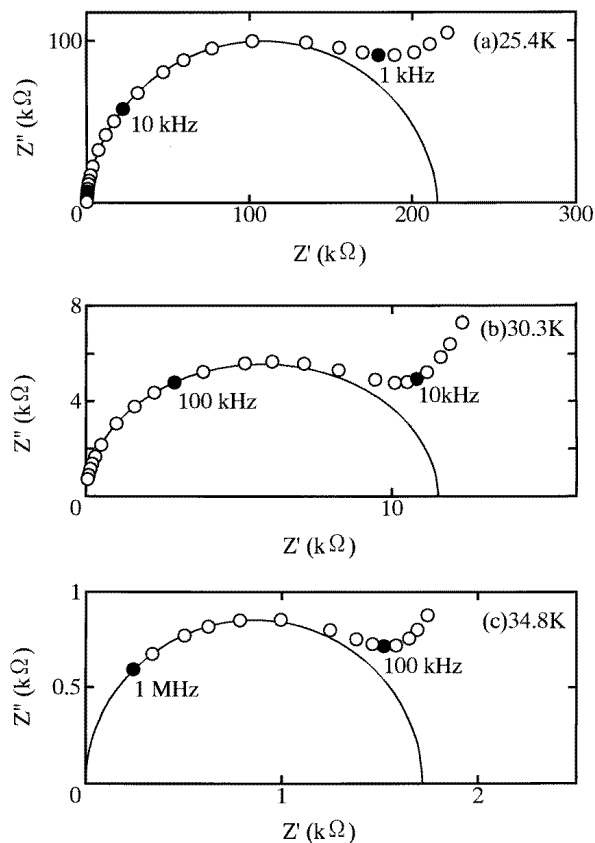


Figure 1. The complex-plane impedance analyses for the $\text{La}_{1-x}\text{Sr}_x\text{CoO}_3$ specimen with $x = 0.03$ at several temperatures: (a) 25.4 K, (b) 30.3 K, and (c) 34.8 K, where Z' and Z'' represent the real and imaginary parts of the total impedance at each applied frequency. The highest resistance value of the highest-frequency arc corresponds to the bulk conduction.

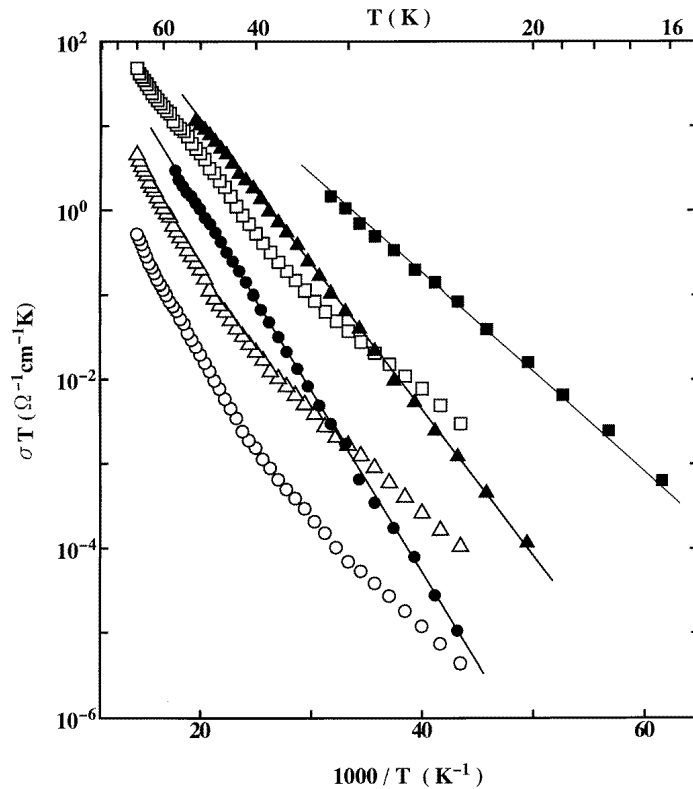


Figure 2. The Arrhenius relations of σT and $1/T$. The solid circles, triangles, and squares show the bulk conductivities obtained by the impedance analyses for the specimens with $x = 0.03$, 0.05 , and 0.07 , and the open circles, triangles, and squares show the dc conductivities measured by the four-probe method for the specimens with $x = 0.03$, 0.05 , and 0.07 . The straight lines represent the linear portions in the Arrhenius plots of the bulk conductivities.

3. Experimental results

Following the detailed account of the theoretical treatment given in [54–57], complex-plane impedance analyses have been carried out. Figure 1 depicts impedance plots at several temperatures for the specimen with $x = 0.03$. The highest-frequency arc corresponding to the bulk conduction is shown for each temperature in figure 1, and the resistance value of the bulk conduction is obtained from the real-axis intercept, i.e., the highest resistance value of this arc. Although the highest-frequency arc appears definitely below around 60 K for the specimens with $x = 0.03$ and 0.05 , and below around 35 K for that with $x = 0.07$, plots of this arc at higher temperatures require frequencies much higher than the maximum one in the present experiment, i.e., 1 MHz. Employing the bulk resistances, figure 2 illustrates the Arrhenius relations of σT and $1/T$. The dc conductivities obtained by the four-probe measurements are also plotted. Theoretically, the four-probe method measures the total resistances in grains and boundaries, and consequently the bulk conductivities are higher than the dc conductivities [54–57]. The dc conduction contains two activated processes for every specimen and the slope changes at around 30 K. Such dc conduction behaviour is very similar to that obtained by Golovanov *et al* [59].

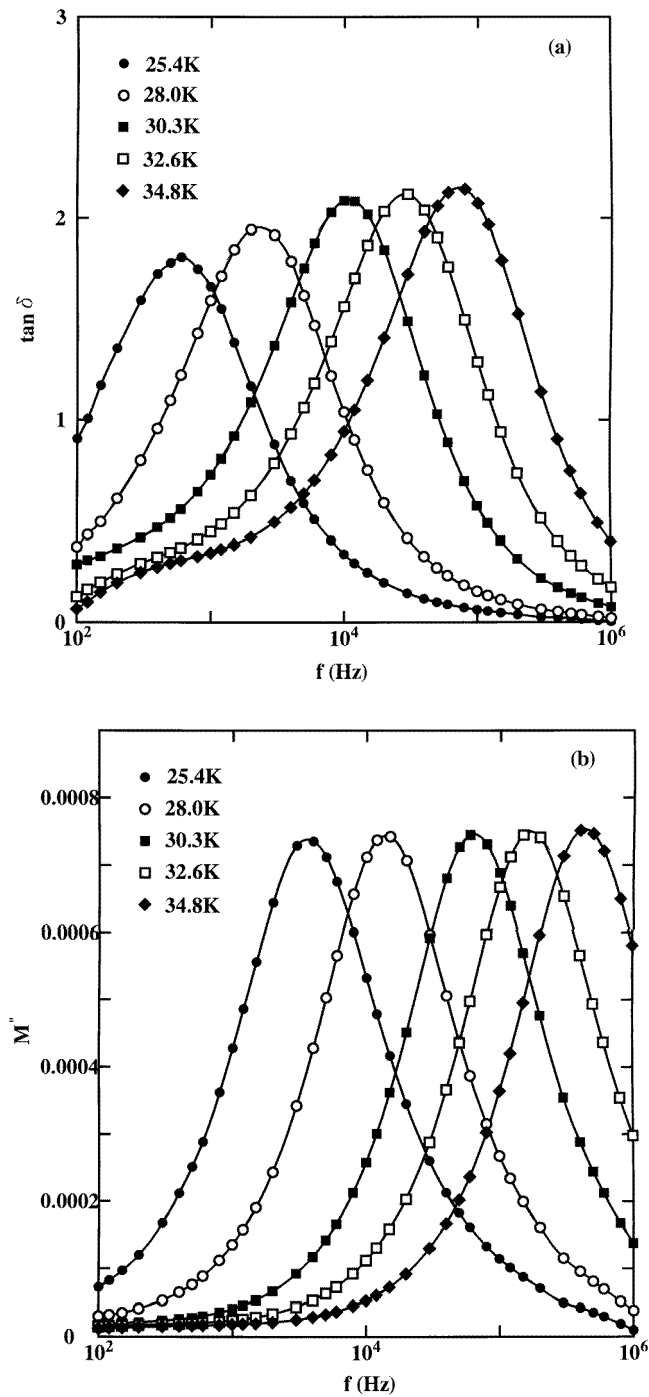


Figure 3. Frequency dependencies of (a) the loss tangent ($\tan \delta$) and (b) the electric modulus (M'') at several temperatures, 25.4 K–34.8 K, for the specimen with $x = 0.03$.

Figure 3 plots dielectric loss tangent ($\tan \delta$) and electric modulus (the imaginary part, M'') as functions of the applied frequency, f , for the specimen with $x = 0.03$ at several temperatures, i.e., 25.4 K–34.8 K. At each temperature, the resonance frequency of the modulus, f_M , is nearly equal to the frequency corresponding to the highest point in the highest-frequency arc in the impedance analysis (see figure 1), f_Z , while the resonance frequency of the loss tangent, $f_{\tan \delta}$, is lower than f_Z . This is due to the fact that the sequence $f_{\tan \delta} < f_Z \leq f_M$ holds when a relaxation process takes place within the grains [60]. The maximum of the loss tangent, $(\tan \delta)_{\max}$, increases with increasing temperature. This behaviour suggests that the spectral intensity of the dielectric relaxation observed in $\text{La}_{1-x}\text{Sr}_x\text{CoO}_3$ is thermally activated, like the dielectric relaxations occurring in various other materials in which processes of hopping of non-adiabatic and/or adiabatic small polarons dominate the electrical transport [46–53].

4. Discussion

4.1. Bulk conduction and dielectric relaxation processes

Each Arrhenius relation for the bulk conductivities gives a good straight line, as shown in figure 2, but the temperatures at which the impedance analyses could be carried out for $\text{La}_{1-x}\text{Sr}_x\text{CoO}_3$ were very low compared with the case for LaCoO_3 [28]. Bulk conductivities markedly higher than the four-probe dc conductivities indicate that the grain boundaries formed in the sintered specimens interfere with the elucidation of the transport phenomena for $\text{La}_{1-x}\text{Sr}_x\text{CoO}_3$. Hence the exclusion of the grain boundary resistances is a minimum requirement for these specimens. As described before, plots of the highest-frequency arcs at higher temperatures require frequencies much higher than the maximum one in the present experiment.

The bulk conductivity increases monotonically with increasing temperature for every specimen as shown in figure 2. The semiconducting $\text{La}_{1-x}\text{Sr}_x\text{CoO}_3$ compound with $x \leq 0.20$ shows a spin-glass regime below the spin-glass-freezing temperature, T_g [34, 35]. $T_g \cong 10, 15,$ and 20 K for $x = 0.03, 0.05,$ and 0.07 [34]. For the specimen with $x = 0.07$, bulk conductivities are obtainable even below $T_g = 20$ K, but there is no anomaly due to spin-glass freezing.

The Arrhenius relations for the bulk conductivities shown in figure 2 are subject to the temperature dependence of the hopping conduction [28], i.e.,

$$\sigma = A_0 \exp(-Q/k_B T)/T$$

where Q is the activation energy required for the conduction. The least-mean-square analyses yield $Q = 0.042, 0.033,$ and 0.021 eV, and $A_0 = 6.5, 6.4,$ and $1.5 \times 10^3 \Omega^{-1} \text{cm}^{-1} \text{K}$ for the specimens with $x = 0.03, 0.05,$ and 0.07 , respectively.

The transport features in figure 2 certainly favour the polaronic scenario of bulk conduction. This is evident from the dielectric properties. The dielectric behaviour shown in figure 3 is described approximately by Debye's theory [60, 61]. At a temperature T , there is a relation

$$(f_{\tan \delta})^2/f_M = \exp(-Q'/k_B T)/2\pi\tau_0$$

where $f_{\tan \delta}$ and f_M are the resonance frequencies for the loss tangent and the electric modulus, Q' is the activation energy required for the dielectric relaxation process, and τ_0 is the pre-exponential term of the relaxation time. Figure 4(a) displays Arrhenius plots of $(f_{\tan \delta})^2/f_M$ and $1/T$. The least-mean-square analyses yield $Q' = 0.039, 0.030,$ and 0.019 eV for the specimens with $x = 0.03, 0.05,$ and 0.07 , respectively.

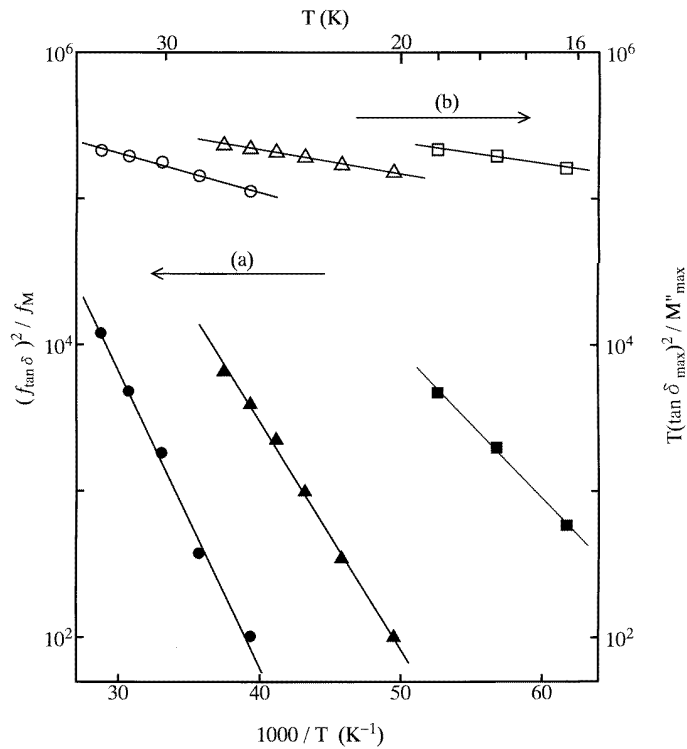


Figure 4. (a) The Arrhenius relation between $(f_{\tan \delta})^2 / f_M$ and $1/T$ (solid circles, triangles, and squares for the specimens with $x = 0.03, 0.05,$ and 0.07), and (b) the Arrhenius relation between $T(\tan \delta_{\max})^2 / M''_{\max}$ and $1/T$ (open circles, triangles, and squares for the specimens with $x = 0.03, 0.05,$ and 0.07).

As shown in figure 3, the maximum of the loss tangent increases with increasing temperature. Such an increase suggests thermal activation in the amount of the hopping carriers, as reported for various oxides [46–53]. There is another dielectric relation

$$T(\tan \delta)_{\max}^2 / M''_{\max} \propto \exp(-W_O / 2k_B T)$$

where $(\tan \delta)_{\max}$ and M''_{\max} are the maxima of the loss tangent and the electric modulus at T [28, 60, 62]. If mobile polarons are created by releasing carriers trapped at imperfections, W_O is the trapping energy. The Arrhenius relations of $T(\tan \delta)_{\max}^2 / M''_{\max}$ and $1/T$ shown in figure 4(b) yield $W_O/2 = 0.005, 0.003,$ and 0.002 eV for the specimens with $x = 0.03, 0.05,$ and 0.07 .

Hence, the sum of Q' and $W_O/2$ is nearly equal to Q for every specimen. When the process of hopping of small polarons dominates the conduction, Q and Q' are represented as $Q = W_H + W_O/2$ and $Q' = W_H$, where W_H is the hopping energy [46–53, 62–64]. In these formulae, the disordered energy is omitted because this is, in general, negligibly small in a crystalline lattice compared with the hopping energy [65]. In comparison with LaCoO_3 , $\text{La}_{1-x}\text{Sr}_x\text{CoO}_3$ exhibits activation energies that are very low. Furthermore, the bulk conduction and the dielectric relaxation processes in $\text{La}_{1-x}\text{Sr}_x\text{CoO}_3$ occur below 60 K, whereas similar processes take place above 120 K in LaCoO_3 . These facts indicate that even a very light Sr doping changes the conduction features, and also alters the nature of the carriers.

4.2. The nature of the charge carriers

On comparison to the results on LaCoO_3 [28, 66], the present study on $\text{La}_{1-x}\text{Sr}_x\text{CoO}_3$ is seen to show several significant points that require accounting for:

(i) the emergence of the hopping conduction in the low-temperature region where the phonon-induced tunnelling effect of small polarons [67] dominates the electrical transport in non-doped LaCoO_3 ;

(ii) the large reduction of the activation energy required for the bulk conduction despite the Sr doping being very slight; and

(iii) the decrease in the activation energy with increasing x .

One should note the following. Hole-doped LaCoO_3 with perovskite-type structure [30, 31] is a member of the group of ferromagnets exhibiting double-exchange interaction [68–70], in which the hole-type carriers in the hybridized 3d–2p bands strongly couple with 3d spins. Although a strong Hund’s rule coupling between the charge carriers (e_g -like states) and the local spins (t_{2g} -like states) determines most of the observable behaviour of hole-doped LaMnO_3 , the absence of a half-filled t_{2g} orbital in the low-spin Co ion gives rise to weaker Hund’s rule coupling of the charge carriers (e_g -like states) to the local spins (t_{2g} -like states) [71]. This is an important fact that distinguishes the hole-doped Co system from the hole-doped Mn system.

In the magnetic experiment on $\text{La}_{1-x}\text{Sr}_x\text{CoO}_3$ carried out by Yamaguchi *et al* [26], the susceptibility drop due to the transition from a high-spin to a low-spin state taking place in LaCoO_3 [15–24] is suppressed, and instead a Curie-like contribution is markedly increased upon a light doping. In fact, even at $x = 0.01$, the susceptibility drop disappears and there is only the Curie-like contribution. Asai *et al* also observed no transition from a high-spin to a low-spin state for $\text{La}_{0.92}\text{Sr}_{0.08}\text{CoO}_3$ in the temperature dependencies of the paramagnetic scattering and the lattice constant obtained by neutron scattering [25]. They ascribe this phenomenon to the lattice expansion induced by the Sr doping, and argue that all or most of the Co ions within the remaining LaCoO_3 matrix in $\text{La}_{0.92}\text{Sr}_{0.08}\text{CoO}_3$ are intermediate-spin Co^{iii} ($t_{2g}^5 e_g^1$) ions [25, 36]. Such susceptibility behaviour in lightly doped LaCoO_3 could be explained by the Curie–Weiss law [32].

In order to check the Curie–Weiss law for the present system, the molar magnetic susceptibilities (χ) of the specimens with $x = 0.03$ and 0.07 were measured as functions of the temperature using a Quantum Design superconducting quantum interference device magnetometer with an applied field of $B = 10$ mT after cooling the specimens in zero field. Figure 5 demonstrates the relationships of χ^{-1} and T . The straight lines at $T > 35$ K for $x = 0.03$ and 80 K for $x = 0.07$ are indicative of a Curie–Weiss law with the formula $\chi = C/(T - \Theta)$, where C is the Curie constant and Θ is the Weiss temperature. If every Co ion is in the intermediate-spin state, i.e., Co^{iii} , $C = 1.00$ emu K mol $^{-1}$ theoretically. On increasing the number of tetravalent Co ions present, the magnitude of the Curie constant increases. The straight lines in figure 5 yield $C = 1.11$ and 1.38 emu K mol $^{-1}$ for $x = 0.03$ and 0.07 . Hence, the content of tetravalent Co ions increases as the hole doping proceeds. This implies that tetravalent Co ions are created by the hole doping, and, moreover, the holes are definitely localized. The least-mean-square analyses yield $\Theta = 11$ and 37 K for $x = 0.03$ and 0.07 , respectively. The deviation from the Curie–Weiss law at low temperatures must be due to the ferromagnetic component which increases with x , but the excessive deviation in the specimen with $x = 0.07$ at around 20 K must contain the contribution of a spin-glass effect in addition to the ferromagnetic effect.

Although an abrupt change in the hopping energy of small polarons on going from

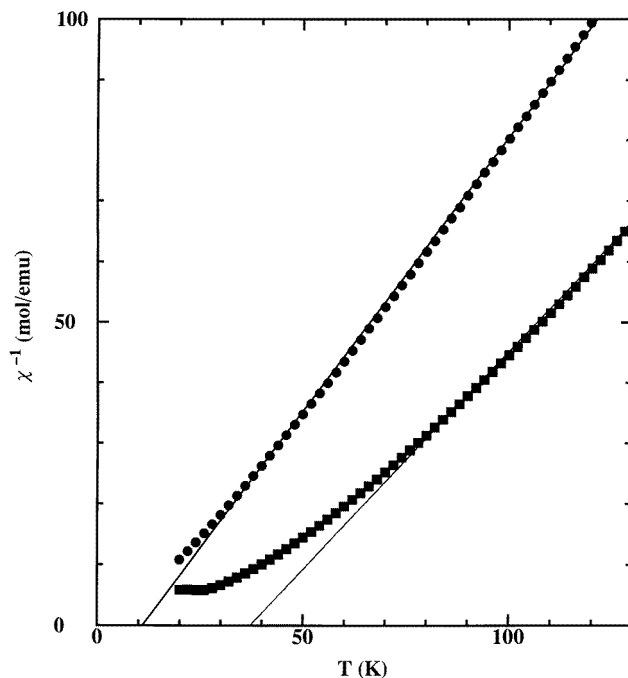


Figure 5. χ^{-1} versus T for the specimens with $x = 0.03$ (solid circles) and 0.07 (solid squares). The straight lines represent the Curie-Weiss laws with $\Theta = 11$ K and 37 K for $x = 0.03$ and 0.07 .

a monovalent system such as LaCoO_3 to a mixed-valence system like $\text{La}_{1-x}\text{Sr}_x\text{CoO}_3$ is normal, one should take account of the peculiar characteristic in $\text{La}_{1-x}\text{Sr}_x\text{CoO}_3$. The most significant difference between LaCoO_3 and $\text{La}_{1-x}\text{Sr}_x\text{CoO}_3$ is as regards the spin state of Co^{3+} . In LaCoO_3 , Co^{3+} ions are in the low-spin state ($\text{Co}^{\text{III}}; t_{2g}^6 e_g^0$) at temperatures below 90 K [29] whereas all or most of the Co^{3+} ions in $\text{La}_{1-x}\text{Sr}_x\text{CoO}_3$ are in the intermediate-spin state ($\text{Co}^{\text{III}}; t_{2g}^5 e_g^1$) [25, 36]. The wave functions of e_g electrons on Co^{III} ions extend straight toward neighbouring O^{2-} ions and e_g electrons have a direct exchange interaction with O^{2-} ions, resulting in the formation of strongly hybridized $3d-2p$ bands. However, t_{2g} electrons in Co^{III} have no direct interaction with O^{2-} ions. Consequently, the bandwidth, $2t'$, of Co^{III} and O^{2-} ions is broad if compared with the very narrow band of Co^{III} and O^{2-} ions in non-doped LaCoO_3 . Since the hopping energy of a small polaron is given as $W_H = W_P/2 - t'$ [62], an increment in t' reduces W_H , where W_P is the polaron binding energy. Although the variation of W_P due to the alternation of the spin state is unknown, the increase in the bandwidth due to the Sr doping must surely be one of the main reasons for the reduction of the hopping energy in $\text{La}_{1-x}\text{Sr}_x\text{CoO}_3$. As x increases, the $3d-2p$ hybridization becomes strong, and accordingly t' increases, leading to a greater reduction of W_H . The tight-binding bandwidth includes the number of nearest neighbours as a factor. The number of directly interacting neighbours for $d_{x^2-y^2}$ parentage of the e_g state is twice that for $d_{3z^2-r^2}$ parentage. Furthermore, the crystal structure of $\text{La}_{1-x}\text{Sr}_x\text{CoO}_3$ being extended along the c -axis implies that the energy level is lower for $d_{x^2-y^2}$ parentage than for $d_{3z^2-r^2}$ parentage. Thus the holes with a strong component of $d_{x^2-y^2}$ parentage move within the lattice by hopping.

Non-doped LaCoO_3 contains only low-spin Co^{III} which does not include e_g electrons at

$T < 90$ K [29]. Since t_{2g} electrons are less hybridized with O 2p states than e_g electrons, hopping motion of small polarons of t_{2g} holes with a rather high activation energy is difficult at low temperatures below 90 K, and instead the phonon-induced tunnelling effect must be predominant in the electrical conduction of LaCoO_3 . As described above, e_g electrons on Co^{iii} ions in $\text{La}_{1-x}\text{Sr}_x\text{CoO}_3$ markedly reduce the hopping energy of small polarons, and consequently the Holstein polaronic model is realized for this material even in the low-temperature region where the phonon-induced tunnelling of polarons occurs in LaCoO_3 .

4.3. Spin polarons

The magnetic properties of lightly Sr-doped LaCoO_3 indicate that the carriers involve a component from a spin polaron [26]. In ferromagnetic insulators, there is a high possibility that carriers are spin polarons. Kasuya and Yanase [72] considered the behaviour of pure spin polarons, defined as carriers localized at impurity centres by polarization clouds, the transport mechanism being thermal hopping between sites. In this picture, the activation energy responsible for the conduction is the energy of the trapping of carriers by impurity centres, i.e., $W_H = W_O$. For $\text{La}_{1-x}\text{Sr}_x\text{CoO}_3$, however, the present study distinguishes the hopping energy from the trapping energy. Mott and Davis [73] argued that the mobility of pure spin polarons was diffusive in nature, i.e., had a power-law temperature dependence rather than a thermally activated one. Their spin polarons are not activated in spite of a diffusive motion and not because of it. In $\text{La}_{1-x}\text{Sr}_x\text{CoO}_3$, however, the hopping process takes place. Emin *et al* [74, 75] considered the nature of lattice polarons in ferromagnetic insulators. In this model, spin polarons are carriers self-localized by the intra-atomic exchange due to the electron–magnon interaction in tandem with the short-range component of the electron–lattice interaction. Hence this model predicts a hopping process to take place.

In the temperature region where the dielectric relaxation due to a hopping process is observed for the present system, a deviation from the Curie–Weiss law occurs as shown in figure 5. This must be due to the ferromagnetic component as described before. Thus the electron–magnon interaction is also expected in this temperature region. According to Kusters *et al* [76], the electron–magnon interaction drives the carriers towards localization, like the electron–lattice interaction, and becomes important particularly at temperatures close to the onset of the ferromagnetism. By analogy with their result, the present system is expected to experience a similar situation, namely both lattice and magnetic characters govern the nature of the charge carrier. The electrical transport in $\text{La}_{1-x}\text{Sr}_x\text{CoO}_3$ at low temperatures is then likely to be rather close to that in the conduction picture constructed by Emin *et al* [74].

The present discussion is based upon a homogeneous intermediate-spin model at temperatures above the spin-glass-freezing temperature, T_g . As regards the specimen with $x = 0.07$, however, the dielectric relaxation process occurs in the spin-glass regime below $T_g = 20$ K (see figure 4), and bulk conductivities are measured even below T_g , as shown in figure 2. The spin-glass regime includes the existence of superparamagnetism and electronic inhomogeneity. Despite this, the Arrhenius bulk conduction follows a straight line, as shown in figure 2, and there is a good correlation between the activation energies for the bulk conduction and the hopping process. These facts must imply that the hopping motion of small polarons is rather insensitive to superparamagnetism and electronic inhomogeneity. In fact, other materials containing spin-glass phases [77, 78] exhibit no peculiarities due to spin-glass freezing in the temperature dependencies of their conductivities, like the specimen with $x = 0.07$. As shown in figure 5, however, the relation of χ^{-1} and T for the specimen with $x = 0.07$ deviates remarkably from the Curie–Weiss law at around $T_g = 20$ K. This

deviation must be closely related to superparamagnetism and electronic inhomogeneity in the spin-glass regime.

4.4. Hopping conduction

Even if electron–magnon interaction occurs to some extent in the present system, the theoretical formulae representing the bulk conduction and the dielectric relaxation process cannot change because electron–lattice interaction is involved. Thus the present experiment yields $W_H = 0.039, 0.030,$ and 0.019 eV for the specimens with $x = 0.03, 0.05,$ and $0.07,$ and $W_O/2 \cong 0.003$ eV for every specimen.

According to Señaris-Rodríguez and Goodenough [35], in the low-doping range the holes initially introduced by substitution of Sr^{2+} for La^{3+} create, formally, low-spin Co^{4+} ions ($\text{Co}^{\text{IV}}; t_{2g}^5 e_g^0$) within a strongly covalent CoO_6 octahedral-site complex. The $\text{Sr}^{2+}\text{--Co}^{\text{IV}}$ states are the trapping sites for holes in $\text{La}_{1-x}\text{Sr}_x\text{CoO}_3$. Under the action of the external field, the trapped holes are thermally excited to the hybridized $3d\text{--}2p$ bands within the remaining LaCoO_3 matrix in $\text{La}_{1-x}\text{Sr}_x\text{CoO}_3$, and move via the bands by hopping.

The polaron theory predicts the following formula for the pre-exponential factor of the conductivity:

$$A_0 = n_0 e^2 \omega_{\text{LO}} a_h^2 / k_B$$

where e denotes the electronic charge, n_0 is the density of Sr^{2+} ions, ω_{LO} is the optical phonon frequency, and a_h is the hopping distance [62–64]. Referring to experiments on the optical frequencies in LaCoO_3 [79], i.e., $\omega_{\text{LO}} = (0.6\text{--}1.9) \times 10^{13} \text{ s}^{-1}$, and employing $a_h =$ the spacing between the centres of cobalt–oxygen bonds because the carrier exhibits strongly the character of a ligand hole, it is now possible to obtain numerical estimates for A_0 : $A_0 = (2\text{--}7) \times 10^3, (4\text{--}11) \times 10^3,$ and $(5\text{--}16) \times 10^3 \text{ } \Omega^{-1} \text{ cm}^{-1} \text{ K}$ for the specimens with $x = 0.03, 0.05,$ and $0.07,$ respectively; these are of the same order of magnitude as the experimental values.

At $T = 60$ K, the magnitudes for W_O yield the densities of the mobile hopping polarons in the range $6 \times 10^{19}\text{--}2 \times 10^{20} \text{ cm}^{-3}$ for the present specimens. Within the remaining LaCoO_3 matrix in $\text{La}_{1-x}\text{Sr}_x\text{CoO}_3$, one should consider another type of conduction reported previously [28], i.e., the hopping conduction of small polarons of holes which are created by electron excitation from O 2p valence bands across the band gap of 0.2 eV. The density of the mobile hopping polarons in this conduction at 60 K is however approximately $1 \times 10^6 \text{ cm}^{-3}$, which is negligibly small in the temperature region investigated in the present study. Consequently, the very small value of W_O for $\text{La}_{1-x}\text{Sr}_x\text{CoO}_3$ must be another reason for the emergence of hopping conduction at considerably lower temperatures than for LaCoO_3 .

Golovanov *et al* [59] reported two thermally activated processes in the dc conduction of $\text{La}_{1-x}\text{Sr}_x\text{CoO}_3$ with $x \leq 0.10$, one above 30 K and another one below 30 K. Their interpretation of the activated process above 30 K is based upon charge transport by hopping, which is consistent with the present study. As shown in figure 2, at temperatures below 30 K, the temperature dependence of the dc conductivity deviates from Arrhenius conduction above 30 K. This is in accord with their result [59]. However, the bulk conduction involves only one thermal process in the temperature region investigated here. Thus the grain boundaries must have a profound effect on the change in the dc conduction feature at 30 K.

5. Conclusions

The electrical transport properties of $\text{La}_{1-x}\text{Sr}_x\text{CoO}_3$ ($0.03 \leq x \leq 0.07$) investigated by complex-plane impedance analyses and dielectric measurements provide evidence of hopping conduction, whose behaviour is however markedly different from the hopping conduction in LaCoO_3 , even though there is only a very small amount of Sr-ion doping. The features in the low-doping range of $\text{La}_{1-x}\text{Sr}_x\text{CoO}_3$ are:

(i) the emergence of the hopping conduction at very low temperatures, i.e., below around 60 K, in comparison with the corresponding temperature region of $300 \text{ K} \geq T \geq 120 \text{ K}$ for non-doped LaCoO_3 ;

(ii) the large reduction of the activation energy required for the conduction, 0.042 eV at $x = 0.03$ to 0.021 eV at $x = 0.07$, from 0.34 eV for LaCoO_3 ; and

(iii) the progressive decrease in the activation energy with increasing x .

Despite the hole doping being light, the susceptibility drop due to the transition from a high-spin to a low-spin state which is characteristic of LaCoO_3 is suppressed, and the magnetic behaviour in the present system is explained by the Curie–Weiss law with a positive value for Θ .

The huge reduction of the activation energy required for the conduction comes from the alternation of the spin state of Co^{3+} caused by the Sr doping. Within the remaining LaCoO_3 matrix in $\text{La}_{1-x}\text{Sr}_x\text{CoO}_3$, all or most of the Co^{3+} ions are in the intermediate-spin state ($\text{Co}^{\text{III}}; t_{2g}^5 e_g^1$), but they are in the low-spin state ($\text{Co}^{\text{III}}; t_{2g}^6 e_g^0$) in non-doped LaCoO_3 at low temperatures. The strong 3d–2p hybridization due to e_g electrons on Co^{III} ions in $\text{La}_{1-x}\text{Sr}_x\text{CoO}_3$ markedly broadens the bandwidth of Co^{III} and O^{2-} , and eventually leads to the large reduction of the activation energy because the bandwidth makes a negative contribution to the activation energy. With increasing x , the hybridized 3d–2p bands become gradually broader, and accordingly the activation energy decreases. Co^{III} ions in non-doped LaCoO_3 have no direct interaction with neighbouring O^{2-} ions, and thus the bands between Co^{III} and O^{2-} are very narrow.

The drastic change in the magnetic properties of $\text{La}_{1-x}\text{Sr}_x\text{CoO}_3$ indicates that the electron–magnon interaction occurs, and drives the carriers towards localization in tandem with the electron–lattice interaction even at temperatures above the Curie point.

Acknowledgments

The authors are very grateful to Professor K Asai, Dr F Munakata, Dr W H Jung, and Dr N Nakamura for their useful advice and discussion of this project. This project was supported by a Grant-in-Aid for Science Research (No 08650812) from the Ministry of Education, Science and Culture, Japan, and also by Takahashi Industrial and Economic Research Foundation.

References

- [1] van Santen J H and Jonker G H 1950 *Physica* **16** 599
- [2] Dougier P and Hagenmuller P 1975 *J. Solid State Chem.* **15** 158
- [3] Webb J B, Sayer M and Mansingh A 1977 *Can. J. Phys.* **55** 1725
- [4] Karim D P and Aldred A T 1979 *Phys. Rev. B* **20** 2255
- [5] Bansal K P, Kumari S, Das B K and Jain G C 1983 *J. Mater. Sci.* **18** 2095
- [6] Grenier J, Ea N, Pouchard M and Abou-Sekkina M M 1984 *Mater. Res. Bull.* **19** 1301
- [7] Lichtenberg F, Widmer D, Bednorz J G, Williams T and Reller A 1991 *Z. Phys. B* **82** 211

- [8] Rajeev K P, Shivashankar G V and Raychaudhuri A K 1991 *Solid State Commun.* **79** 591
- [9] Sreedhar K, Hoing J M, Darwin M, McElfresh M, Shand P M, Xu J, Crooker B C and Spalek J 1992 *Phys. Rev. B* **46** 6382
- [10] Tokura Y, Taguchi Y, Okada Y, Fujishima Y, Arima T, Kumagai K and Iye Y 1993 *Phys. Rev. Lett.* **70** 2126
- [11] Sarma D D and Chainani A 1994 *J. Solid State Chem.* **111** 208
- [12] Sarma D D, Shanthi N, Barman S R, Hamada N, Sawada H and Terakura K 1995 *Phys. Rev. Lett.* **75** 1126
- [13] Arima T and Tokura Y 1995 *J. Phys. Soc. Japan* **64** 2488
- [14] Mahadevan P, Shanthi N and Sarma D D 1996 *Phys. Rev. B* **54** 11 199
- [15] Koehler W C and Wollan E O 1957 *J. Phys. Chem. Solids* **2** 100
- [16] Heikes R R, Miller R C and Mazelsky R 1964 *Physica* **30** 1600
- [17] Naiman C S, Gilmore R, Dibartolo B, Linz A and Santoro R 1965 *J. Appl. Phys.* **36** 1044
- [18] Jonker G H 1966 *J. Appl. Phys.* **37** 1424
- [19] Raccach P M and Goodenough J B 1967 *Phys. Rev.* **155** 932
- [20] Menyuk N, Dwight K and Raccach P M 1967 *J. Phys. Chem. Solids* **28** 549
- [21] Bhide V G, Rajoria D S, Rao G R and Rao C N R 1972 *Phys. Rev. B* **6** 1021
- [22] Asai K, Gehring P, Chou H and Shirane G 1989 *Phys. Rev. B* **40** 10982
- [23] Chainani A, Mathew M and Sarma D D 1992 *Phys. Rev. B* **46** 9976
- [24] Abbate M, Fuggle J C, Fujimori A, Tjeng L H, Chen C T, Potze R, Sawatzky G A, Eisaki H and Uchida S 1993 *Phys. Rev. B* **47** 16 124
- [25] Asai K, Yokokura O, Nishimori N, Chou H, Tranquada J M, Shirane G, Higuchi S, Okajima Y and Kohn K 1994 *Phys. Rev. B* **50** 3025
- [26] Yamaguchi S, Okimoto Y, Taniguchi H and Tokura Y 1996 *Phys. Rev. B* **53** R2926
- [27] Korotin M A, Ezhov S Y, Solov'yev I V, Anisimov V I, Khomskii D I and Sawatzky G A 1996 *Phys. Rev. B* **54** 5309
- [28] Iguchi E, Ueda K and Jung W H 1996 *Phys. Rev. B* **54** 17 431
- [29] Saitoh T, Mizokawa T, Fujimori A, Abbate M, Takeda Y and Takano M 1997 *Phys. Rev. B* **55** 4257
- [30] Jonker G H and van Santen J H 1953 *Physica* **19** 120
- [31] Raccach P M and Goodenough J B 1968 *J. Appl. Phys.* **39** 1209
- [32] Bhide V G, Rajoria D S, Rao C N R, Rama Rao G and Jadhao V G 1975 *Phys. Rev. B* **12** 2832
- [33] Rao C N R, Parkash Om, Bahadur D, Ganguly P and Nagabhushana S 1977 *J. Solid State Chem.* **22** 353
- [34] Itoh M, Natori I, Kubota S and Motoya K 1994 *J. Phys. Soc. Japan* **63** 1486
- [35] Señaris-Rodríguez M A and Goodenough J B 1995 *J. Solid State Chem.* **118** 323
- [36] Asai K 1997 private communication
- [37] Menyuk N, Raccach P M and Dwight K 1968 *Phys. Rev.* **166** 510
- [38] Taguchi H, Shimada M and Koizumi M 1978 *Mater. Res. Bull.* **13** 1225
- [39] Taguchi H, Shimada M and Koizumi M 1980 *Mater. Res. Bull.* **15** 165
- [40] Sathe V G, Pimpale A V, Siruguri V and Paranjpe S K 1996 *J. Phys.: Condens. Matter* **8** 3889
- [41] Ganguly P, Anil Kumar P S, Santhosh P N and Mulla I S 1994 *J. Phys.: Condens. Matter* **8** 533
- [42] Mahendiran R, Raychaudhuri A K, Chainani A and Sarma D D 1995 *J. Phys.: Condens. Matter* **7** L561
- [43] Mansingh A, Reyes J M and Sayer M 1972 *J. Non-Cryst. Solids* **7** 12
- [44] Gehlig R and Salje E 1983 *Phil. Mag.* **B 47** 229
- [45] Sidek H A A, Collier I T, Hampton R N, Saunders G A and Bridge B 1989 *Phil. Mag.* **B 59** 221
- [46] Iguchi E, Kubota N, Nakamori T, Yamamoto N and Lee K J 1991 *Phys. Rev. B* **43** 8646
- [47] Iguchi E and Akashi K 1992 *J. Phys. Soc. Japan* **61** 3385
- [48] Lee K J, Iguchi A and Iguchi E 1993 *J. Phys. Chem. Solids* **54** 975
- [49] Iguchi E and Jung W H 1994 *J. Phys. Soc. Japan* **63** 3078
- [50] Jung W H and Iguchi E 1995 *J. Phys.: Condens. Matter* **7** 1215
- [51] Iguchi E, Hashimoto T and Yokoyama S 1996 *J. Phys. Soc. Japan* **65** 221
- [52] Jung W H and Iguchi E 1996 *Phil. Mag.* **B 73** 873
- [53] Iguchi E, Nakamura N and Aoki A 1997 *J. Phys. Chem. Solids* **58** 755
- [54] MacDonald J R 1974 *J. Chem. Phys.* **61** 3977
- [55] MacDonald J R 1976 *Superionic Conductors* ed S D Mahan and W L Roth (New York: Plenum) p 81
- [56] Bauerle J E 1969 *J. Phys. Chem. Solids* **30** 2657
- [57] Franklin A D 1975 *J. Am. Ceram. Soc.* **58** 465
- [58] Bednorz J G and Müller K A 1986 *Z. Phys.* **B 64** 189
- [59] Golovanov V, Mihaly L and Moodenbaugh A R 1996 *Phys. Rev. B* **53** 8207
- [60] Gerhardt R 1994 *J. Phys. Chem. Solids* **55** 1491
- [61] Frölich H 1958 *Theory of Dielectrics* (Oxford: Clarendon) p 70

- [62] Austin I G and Mott N F 1969 *Adv. Phys.* **18** 41
- [63] Lang I G and Firsov Yu A 1968 *Zh. Eksp. Teor. Fiz.* **54** 826
- [64] Emin D and Holstein T 1969 *Ann. Phys., NY* **53** 439
- [65] Dominik L A K and MacCrone R K 1967 *Phys. Rev.* **163** 756
- [66] Senáris-Rodríguez M A and Goodenough J B 1995 *J. Solid State Chem.* **116** 224
- [67] Holstein T 1959 *Ann. Phys., NY* **8** 343
- [68] Zener C 1951 *Phys. Rev.* **82** 403
- [69] Anderson P W and Hasegawa H 1955 *Phys. Rev.* **100** 675
- [70] de Gennes P G 1960 *Phys. Rev.* **118** 141
- [71] Mahendiran R and Raychaudhuri A K 1996 *Phys. Rev. B* **54** 16044
- [72] Kasuya T and Yanase A 1968 *Rev. Mod. Phys.* **40** 684
- [73] Mott N F and Davis E A 1979 *Electronic Processes in Non-Crystalline Materials* 2nd edn (Oxford: Oxford University Press) p 156
- [74] Emin D, Hilley M S and Liu N H 1986 *Phys. Rev. B* **33** 2933
- [75] Emin D, Hilley M S and Liu N H 1987 *Phys. Rev. B* **35** 641
- [76] Kusters R M, Singleton J, Keen D A, McGreevy R and Hayes W 1989 *Physica B* **155** 362
- [77] Mydosh J A 1974 *Phys. Rev. B* **10** 2845
- [78] Ford P J and Mydosh J A 1976 *Phys. Rev. B* **14** 2057
- [79] Tajima S, Masaki A, Uchida S, Matsuura T, Fueki K and Sugai S 1986 *J. Phys. C: Solid State Phys.* **20** 3469